IOPscience iopscience.iop.org

Home Search Collections Journals About Contact us My IOPscience

Are global wind power resource estimates overstated?

This article has been downloaded from IOPscience. Please scroll down to see the full text article.

2013 Environ. Res. Lett. 8 015021

(http://iopscience.iop.org/1748-9326/8/1/015021)

View the table of contents for this issue, or go to the journal homepage for more

Download details:
IP Address: 199.21.102.236
The article was downloaded on 26/02/2013 at 18:03

Please note that terms and conditions apply.

OPEN ACCESS
IOP PUBLISHING
ENVIRONMENTAL RESEARCH LETTERS
Environ. Res. Lett. **8** (2013) 015021 (9pp)
doi:10.1088/1748-9326/8/1/015021

Are global wind power resource estimates overstated?

Amanda S Adams[1] **and David W Keith**[2]

[1] Department of Geography and Earth Sciences, University of North Carolina at Charlotte, 9201 University City Blvd, Charlotte, NC 28223, USA
[2] School of Engineering and Applied Sciences, Harvard University, 29 Oxford St, Cambridge, MA 02138, USA

E-mail: david_keith@harvard.edu

Received 4 July 2012
Accepted for publication 15 January 2013
Published 25 February 2013
Online at stacks.iop.org/ERL/8/015021

Abstract
Estimates of the global wind power resource over land range from 56 to 400 TW. Most estimates have implicitly assumed that extraction of wind energy does not alter large-scale winds enough to significantly limit wind power production. Estimates that ignore the effect of wind turbine drag on local winds have assumed that wind power production of 2–4 W m^{-2} can be sustained over large areas. New results from a mesoscale model suggest that wind power production is limited to about 1 W m^{-2} at wind farm scales larger than about 100 km^2. We find that the mesoscale model results are quantitatively consistent with results from global models that simulated the climate response to much larger wind power capacities. Wind resource estimates that ignore the effect of wind turbines in slowing large-scale winds may therefore substantially overestimate the wind power resource.

Keywords: wind power, energy, environmental impact, resource estimation

1. Introduction

Wind turbines extract kinetic energy from the mean flow and produce a plume of low velocity air downstream. At the local scale it is well understood that wind turbines cannot be spaced too closely together or the power extracted per turbine will decrease driving up the amortized cost of electricity. At the scale of typical commercial wind farms, which rarely have more than a few rows of turbines along the prevailing wind direction, turbines are typically spaced 5–10 rotor diameters apart, equivalent to a density of 2–10 MW of installed wind turbine capacity per square kilometer, or a peak power output of 2–10 W m^{-2} of land surface area [1].

Estimates of regional or global wind power capacity generally produced by simply summing local wind power capacity assume that wind farms are deployed at some given areal density. That is to say the wind turbines are spaced at a particular interval (which may be a function of mean wind speed). In some studies this wind turbine density may be further constrained by proximity to energy demand and perhaps other economic and geographic factors [2–4]. The total wind power resource is then computed by multiplying this capacity density by the capacity factor (CF) defined as the ratio of actual power production given the prevailing winds to the amount that would be produced if the turbines operated continuously as their maximum rated output. We will use capacity density (CD) to describe the areal density of a wind turbine array as measured by the rated maximum turbine output per unit land surface area and production density (PD) to denote the average electrical production per unit land surface area, so that PD = CF × CD. While CD is typically expressed as MW km^{-2} we will use W m^{-2} for both CD and PD.

Large-scale deployment of wind turbines may be expected to slow local winds, reducing CF and so reducing total wind power that can be extracted. Previous estimates of regional or global wind power resources [2–4] have ignored this effect, by assumed that array efficiency is independent

Content from this work may be used under the terms of the Creative Commons Attribution 3.0 licence. Any further distribution of this work must maintain attribution to the author(s) and the title of the work, journal citation and DOI.

 © 2013 IOP Publishing Ltd Printed in the UK

of total capacity, and have therefore neglected the large-scale atmospheric energetics that constrain global winds and so constrain the energy they can be extracted by wind turbine arrays. Here we show that estimates based only on local wind power constraints may substantially overestimate global wind power capacity, by overestimating the CF's that could actually be obtained.

Most of the kinetic energy that drives surface winds originates with the generation of available potential energy (APE) at planetary scales by factors such as the pole-to-equator gradient in diabatic heating [5, 6]. The generation of APE at large-scales cascades downwards and fuels winds throughout the atmosphere. Within the atmospheric boundary layer, turbulent mixing transports momentum downward to the surface and converts kinetic energy to heat via viscous (frictional) dissipation. The globally averaged dissipation of kinetic energy is about 1.9 W m^{-2}, and almost all of that dissipation occurs as surface friction or gravity wave breaking in the upper atmosphere [6]. The small downward flux of kinetic energy ultimately limits the power that can be extracted by wind turbine arrays [7].

Consider wind turbines distributed evenly over some area. When the CD is sufficiently low its effect on winds within the area can be neglected and PD will increase linearly with the turbine density so that CF is constant. However, as the turbine density increases winds must slow and CF must decline so that PD grows sub-linearly. At sufficiently high PD the power produced will reach a maximum and then decrease as the increasing turbine density slows the winds.

In section 2 we review prior estimates of global wind resource almost all of which assume a linear relationship between CD and PD. In section 3 we describe a parameterization of wind turbine arrays within a mesoscale model; and then in section 4 we use results from this model along with prior results from a global models to explore the response of PD to increasing CD. The plausibility of prior global capacity estimates that ignore effect of wind turbines in slowing winds hangs on the implicit assumption that PD is sufficiently small that the non-linearity of PD with CD can be ignored. Our review in section 2 therefore pays particular attention to the PDs used in such resource estimates. Finally, in the discussion in section 5, we speculate about how more realistic estimates of wind resource might be obtained.

2. Estimates of global wind capacity

Grubb and Meyer [3] produced an early (1993) estimate of global wind energy potential. Their 'first order' estimate assumed that 23% of the world's land area is suitable for wind power extraction and that the average conversion efficiency of wind power to electricity was 26%, which in turn assumed a base 35% CF to which they applied array and system losses of 25%. They study used a turbine spacing of 10 × 5 rotor diameters with 50 m diameter turbines (∼750 kW capacity per turbine) resulting in a capacity density (CD) of 6 W m^{-2} and a wind power production density (PD) of 1.6 W m^{-2}. The resulting estimate of global wind power resource was 56 TW. Note that here and throughout wind power resource estimates refer to annual mean electrical power. While the Grubb and Meyer estimate includes losses due to turbine interactions in arrays, it does so with a single uniform reduction in capacity factor that is independent of the total capacity.

More recently, Archer and Jacobson [2] developed a systematic evaluation of wind speed data from surface, buoy and sounding observations and used the data to estimate wind speeds at wind turbine hub height. With this data set, they estimated the global wind power capacity by restricting the capacity estimate to areas with class 3 wind resources (mean wind speeds >6.9 ms^{-1}) or better. The resulting wind power resource estimate was ∼72 TW over 12.7% of the Earth's land surface.

Archer and Jacobson assumed that wind power is extracted from all areas with class 3 or better winds using a uniform capacity density of 9 W m^{-2}, and assume a uniform capacity factor (*CF*) of 48% for a wind power production density of 4.3 W m^{-2}.

While CF's exceeding 48% have been observed at individual wind turbines, a large-scale average CF of 48% it is not plausible. First, as we will demonstrate below, wind turbine arrays slow local winds greatly reducing CF's at installed turbine density as large as that assumed by Archer and Jacobson. Second, even at low turbine densities where one can ignore the reduction in wind speeds average CFs are not likely to approach 48%. The majority of wind farms sampled by the US Department of Energy between 1998 and 2005, for example, had CFs between 25–35% and very few were over 40% [8]. Similarly, using hourly data from all the wind farms in Texas which has the largest wind capacity in the US over 2007–2008 the average CF was only 27.8 [9]. The US National Energy Modeling System assumes a maximum CF for onshore wind of 40% in 2010 growing to 46% in 2030 [10].

Lu *et al* [4] provided an updated estimate of global wind capacity in 2009. They used global wind field simulations from Goddard Earth and Observing System Data Assimilation System (GEOS-5 DAS) to improve on the global wind energy potential estimate of Archer and Jacobson [2]. The GEOS-5 DAS winds were produced from a global meteorological reanalysis which included not only surface, buoy, and sounding measurements used by Archer and Jacobson but also observations from aircraft, balloons, ships, satellites, and dropsondes. Lu *et al* used the high resolution GEOS-5 DAS from 2006 to estimate winds at 100 m, the approximate hub height modern 2–4 MW class turbines.

Lu *et al* [4] assumed a uniform capacity density of 8.9 W m^{-2} for onshore and 5.8 W m^{-2} for offshore. Improving on Archer and Jacobson, Lu *et al* computed the CF from their wind data, and then estimated total wind resources as a function of the lowest value of CF allowed in order to account for the fact that low CFs are less economic. The annual average onshore wind potential was estimated as high at 7.2 W m^{-2} in some locations, corresponding to a CF of 81%. The resulting global wind energy potential was 148 TW with no CF limit and 96 TW for $CF > 20\%$.

Lu *et al* do not provide a mean CF for the 148 TW case. Using their data the state level estimates of annual energy

generation potential expressed in TWh, one can compute that the average power densities were over 2 W m^{-2} in states such as Kansas, North Dakota, South Dakota, Oklahoma, Nebraska and Iowa. Considering those were the average power densities across an entire state, and it is safe to assume that those state averages are based on the turbines being placed only in areas with good wind resources, it seems that the expected power densities on which the Lu *et al* estimate is based are likely considerably higher than 2 W m^{-2}.

Archer and Jacobson do not mention the possibility that the large-scale collective effects of the wind turbines could limit the extracted energy. Lu *et al* mention that because the total energy dissipated in surface friction is limited by large-scale generation of kinetic energy, 'An increase in friction caused by the presence of the turbines is likely to be compensated by a decrease in frictional dissipation elsewhere', but they do not quantify the effect or provide any physical argument why is can be dismissed. Grubb and Meyer mention array losses, but their assumptions are based on small arrays (10 × 10 at largest) and should not be expected to account for interactions in a global wind capacity estimate.

Finally, while this paper was under review, two recent papers have examined wind power capacity using general circulation models (GCM) that do account for dissipation of energy. As seen in figure 2 of Keith *et al* [11], the wind power production in a GCM does not grow linearly with wind power capacity but rather saturates at some point where the added power generated by additional turbines is matched by the loss of power due to the reduction in wind speeds caused by the addition capacity. Jacobson and Archer [12] found a saturation global capacity of 72 TW over the entire global land surface (excluding Antarctica) in sharp contrast with results from the earlier Archer and Jacobson [2] paper that ignored collective effects and estimated a capacity of 72 TW over just 12.7% of the global land surface. Similarly, Marvel *et al* [13] used a GCM with an added drag term to explore the maximum amount of extractable energy and found a maximum of 400 TW over entire global surface (land and ocean). This value may be consistent with Jacobson and Archer's estimate of 253 TW over the global surface when one considers the ratio of electricity production to energy dissipation, the 'atmospheric efficiency', which Keith *et al* estimate is roughly 50%.

3. Parameterization of wind turbines in a mesoscale model

Previous modeling studies of the influence of wind power extraction have focused on the understanding the magnitude and scale of climatic impacts using either global models [11, 13–15], or mesoscale models [16–20]. Our focus is on understanding how the reduction in wind speed due to wind turbines scales with the size and density of a wind turbine array so we can assess how important the consequent reduction in capacity factor is to estimates of the wind resource.

We make use of a parameterization[3] [21] of the atmospheric effects of wind turbine arrays developed for use in a mesoscale model. We chose a mesoscale model over a GCM or a large eddy simulation (LES) model because a mesoscale model allows for nested grids, heterogeneous forcing based on real atmospheric conditions, and the treatment of boundary layer physics on a scale appropriate for the question at hand. We used the Weather Research and Forecasting Advanced Research model (WRF-ARW, v2.2) [22] because it is a community standard model for mesoscale modeling for research purposes, and because WRF-ARW will, in future studies, allow us to nest a LES model within the mesoscale model.

The wind farm parameterization is used with either of two boundary layer parameterizations, Mellor Yamada Janjic (MJY) [23] and Yonsei University (YSU) [24]. While wind farms could be considered a change in land use, the hub height of modern wind turbines is tall enough to extend beyond the lowest grid box, especially in simulations with high vertical resolution, and thus the modifications to WRF were implemented in the PBL (Planetary Boundary Layer) scheme rather than the surface or land use scheme. This also allowed the mesoscale model to maintain the differences in underlying vegetation, as wind farms are developed on a variety of land types.

The parameterization is based on observed velocity-dependant drag coefficient of wind turbines. It does not resolve individual turbines and is designed to be independent of vertical and horizontal model resolution. This scale-independence is accomplished by defining a wind turbine density for each grid box that represents the area swept by the turbines per grid box volume and has units of inverse length (m^{-1}). The wind turbine density thus takes into account both the horizontal density of the wind turbines as well as the fraction of the turbine blade that is in a grid box vertically. The wind turbine density of each grid box is given by:

$$\Psi = \frac{\left(z\sqrt{r^2 - z^2} + r^2 \arcsin\left(\frac{z}{r}\right)\right) N_{\mathrm{T}}\, \Delta x\, \Delta y}{\Delta x\, \Delta y\, \Delta z} \qquad (1)$$

where Ψ = wind farm density (m^{-1}); r = rotor radius (m); N_{T} = number of turbines km^{-2}; Δx, Δy, Δz = grid box size in each dimension.

The parameterization is 'scale independent' in the sense that by treating the physically discrete wind turbines as a continuous distribution the average wind turbine density is maintained as the model resolution is changed. This improves on some prior parameterizations, but it cannot—of course—ensure that the model results are independent of scale. At small horizontal scales, where the horizontal grid spacing becomes equal to or smaller than the rotor diameter, the parameterization would not be appropriate. However, at those small horizontal scales a PBL scheme would not be appropriate and thus an LES should be employed.

The parameterization conserves energy and momentum. The energy removed from the atmosphere by the turbines can

[3] Model code is available from the authors on request. We expect to make this parameterization available in a future WRF release.

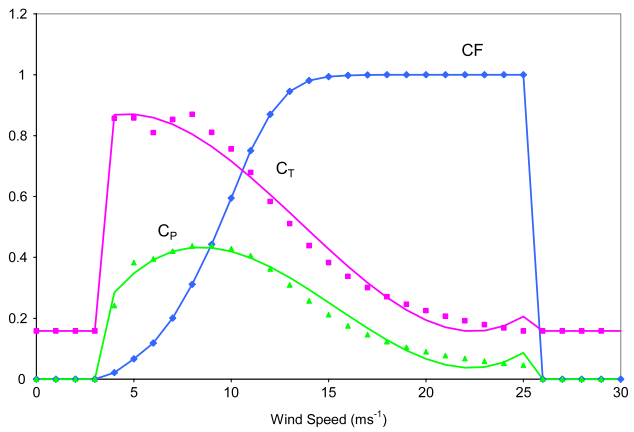

Figure 1. Thrust coefficient (C_T) and power coefficient (C_P) used in the wind turbines parameterization. Data (dots) is from a 2.0 MW bonus energy wind turbine [25]. Solid lines are the thrust and power coefficients used in the parameterization which are derived from a piecewise polynomial fit of the data. The capacity factor (CF) is added for reference though it is not directly used in the parameterization. Note that the polynomial fit is imperfect, but the errors in the middle of the wind speed range are comparable to the uncertainty in the data.

be expressed as a drag force per unit area:

$$\vec{F}_{\text{drag}} = \tfrac{1}{2} C_T \rho \psi v^2 \tag{2}$$

where C_T is a wind-speed-dependent thrust coefficient (see figure 1), ρ is the air density, ψ is the wind farm density and v is the wind velocity.

The drag force produces a sink of kinetic energy. The energy removed from the resolved flow by the wind turbines goes into (i) electricity, (ii) frictional heat loss due to mechanical workings, or (iii) back into the atmosphere in the form of turbulent kinetic energy (TKE). Electricity production is given by:

$$P_e = \tfrac{1}{2} C_P \rho \psi v^3 \tag{3}$$

where C_P is a wind-speed-dependent power coefficient (figure 1). The amount of energy that goes into mechanical losses and TKE is not fully known. We assume that the mechanical losses are negligible and the amount of energy added to the TKE is given by:

$$P_{\text{TKE}} = \tfrac{1}{2} C_{\text{TKE}} \rho \psi v^3 \tag{4}$$

$$C_{\text{TKE}} = C_T - C_P. \tag{5}$$

The thrust, power, and TKE coefficients depend on wind speed as well as on the specific turbine design. Similarly the wind farm density term (ψ), depends on the turbine specifications such as hub height and rotor diameter. We used specifications from a Bonus Energy A/S 2.0 MW turbine, which is representative of modern wind turbines (figure 1). The 2.0 MW turbine specifications include: a hub height of 60 m, a turbine diameter of 76 m, a cut-in speed of 4 ms^{-1}, a cut-out speed of 25 ms^{-1}, and a standing thrust coefficient of 0.158. The thrust coefficient (C_T) and power curve were obtained through WAsP (the Wind Atlas Analysis and Application Program) a program maintained by Danish Technical University [25]. The power curve was used to derive the power coefficient (C_P). A polynomial fit was used in the parameterization to describe the C_T and C_P curves. The cut-in speed and cut-out speeds represent the range of wind speeds at which the wind turbines operate. Below the cut-in speed and above the cut-out speed the standing thrust coefficient is used, and since no electricity is generated all of the energy removed from the resolved flow is converted into a TKE source.

This force-based grid-scale approach is consistent with physical parameterizations in mesoscale models such as WRF. There may be situations in which higher resolution and use of large eddy simulation physics would be appropriate, but if the model scale is such that individual wakes cannot be represented, as is the case here, then the parameterization must in the end specify the net force exerted by all of the turbines within the grid box.

Wind speeds drop within large wind turbine arrays due to the drag forces [21]. Our parameterization assumes that the wind is constant within a grid box, thus the parameterization will tend to overestimate drag if the model resolution is such that there are many turbines within each grid box, or more precisely a ψ sufficiently large that there are large decreases in wind speed over a single grid box. One may think of the entire first grid box at the upstream end of a wind farm as like a first row of turbines although the grid box might (depending on the density) be representing multiple rows of turbines in our parameterization. In practice this error is small at the turbine densities used in our simulations. Additionally, the parameterization uses a single uniform wind speed for each vertical level. Wind turbines do in fact produce electricity that differs from what would be predicted by the power rating and wind speed at hub height because of wind shear, but our parameterization treats each grid box as spatially uniform.

The simulations used a series of 3 nested grids at 90, 30 and 10 km horizontal resolution and 27 vertical levels. The choice of 27 vertical levels results in the wind turbines residing in the two lowest grid boxes. Two-way nesting was used so changes in the inner grids were propagated back to larger scales. Boundary conditions were imposed at the outer grid every 6 h using data from the global forecasting system final analysis (GFS-FNL). The Kain–Fritsch cumulus parameterization was used on grids 1 and 2. Other parameterization choices used were the Lin *et al* [26] microphysics scheme, the RRTM scheme for longwave radiation, and the Dudhia scheme for shortwave radiation [22]. The 3rd order Runge–Kutta scheme was used for the time differencing.

4. Results

To examine the effect of the scale and density of wind turbine arrays, we ran a series of simulations using turbine arrays of three sizes, 2.7, 30 and 270 $\times$ 10^3 km^2 (which we denote 'small', 'medium' and 'large' referring to the areal coverage) and with capacity densities (CDs) ranging from 0.5 to 32 W m^{-2}. The area and CD configurations used in the small, medium and large runs, all use the same 10 days of

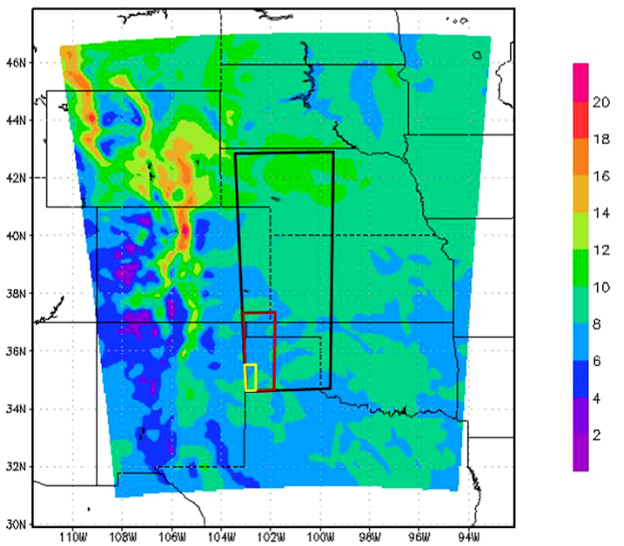

Figure 2. Average wind speed (ms^{-1}) from January 5 to 15 2006 at hub height on grid 3 taken from the control run. Wind speeds through out the central plains were representative of good wind resources for this period. The locations of the 'small', 'medium', and 'large' wind farms are indicated in yellow, red and black respectively.

the GFS-FNL data to initialize the model and to determine the outer boundary condition, starting 5 January 2006. A ten day period was initially chosen as the minimum period to allow the simulation to sample a variety of atmospheric states (e.g., stability, wind speed) and is more than sufficient time for wind to flow through even the largest wind farm under the lowest observed mean wind speed. The average wind speeds at hub height from the control run, on the inner most grid, are shown in figure 2.

Figure 3 shows a comparison between a medium and large wind turbine array with capacity densities of 4 and 0.5 W m^{-2}, each with approximately the same total capacity, (120 and 135 GW respectively). The decrease in the wind speed cubed (horizontal energy flux) is far larger in the high-density medium array than in the large low-density case (top row of figure 3). The difference in the wind speed cubed is plotted rather than the difference in the wind speed, because at CF's of less than 100% the electricity generated is a function of primarily the wind speed cubed. The average wind speeds at hub height in the control run in the region of the wind farms was less than 10 ms^{-1}, and thus well below the wind speed required to reach a 100% CF.

The wind farm with a CD of 4 W m^{-2} shows a decrease in wind speed of approximately 40%. This is consistent with Barthelmie *et al* [27] who observed winds in two wind farms and showed that rows of turbines downwind produced electricity at an average of about 60% of the production in the first upstream row. The spacing of the turbines in the wind farms examined by Barthelmie *et al* is closest to our 4 W m^{-2} CD. The observed reduction in output depended on wind direction with downwind electricity production varying between about 50–60%. For some wind directions (3 of the 7 examined) Barthelmie *et al* [27] show the Horns Rev wind farm has a trend of continuing reduction all the way to the end of the wind farm. Many of the CDs examined in this paper are higher than the wind farms observed by Barthelmie *et al* so a direct comparison across the full range of our results is not possible. Modeling results of Fitch *et al* [20] show power output decreases to a minimum of 65% of the most productive turbines, for a 10 km by 10 km wind farm simulated in an idealized framework, with a turbine spacing of 8 rotor diameters ($CD = 5$ W m^{-2}). Fitch *et al* [20] note that the turbines producing the least amount of electricity are on the farthest downstream edge of their simulated wind farm, thus it is possible that if their wind farm was larger in size they would have seen an even larger reduction in production. However, despite the difference in scale, our results are similar to those of Fitch *et al* [20]. Note that we chose CDs to (a) sample a range of CDs, (b) model CDs that are assumed in prior estimates of the global wind resources, and (c) to assess the limit to energy extraction as CD increases.

The predicted capacity factors (CF's) calculated from a control run without the influence of wind turbine drag are 28.5% and 21.9% for the large and medium arrays respectively; while in the interactive model, wind turbine drag reduces the *CF's* to 26.3% and 12.1%. While hypothetical turbine arrays are far larger than any current wind farm, the 4 W m^{-2} CD used in the medium array is typical of that used in most of the large-scale wind resource calculations described in section 1. It is evident that the spacing of the turbines is critical for maximum energy production from wind, and that the collective effect of wind turbines can play a strong role in limiting wind power extraction at these scales.

The capacity factor in the low-density scenario which ignores collective effects (control run) is somewhat smaller than achieved by many commercial wind farms today. This makes sense as real wind turbines are very carefully sited to optimize capacity factor given local topographic features and wind resource variability whereas the modeled turbines are, in effect, evenly spaced. Also, in the mesoscale model, there is just one wind speed for all turbines in a given grid box, where in reality there would be variations in wind speed between turbines in a 10×10 km^2 area. So we are basing the capacity factor on average wind speeds, and since the electricity produced depends on the wind speed cubed, this coarse grid spacing allows for an underestimate of electricity produced in areas that would in reality have higher wind speeds than the average wind speed. The even-spacing assumption may be realistic for large-scale wind resource studies, because at the very large total wind capacities contemplated, there would be less opportunity to choose the best possible sites.

Figure 4 shows results from the complete series of experiments (see table 1 for a description of simulations performed), plotted so as to display the reduction in capacity factor due to the collective effect of wind turbine arrays in slowing ambient winds. The actual energy produced is compared to the amount that would be expected using winds in the control run, that is, without collective effects. The *x*-axis reflects not only the CD used in each simulation, but also the CF based on the wind speeds of the control run. Thus the *x*-axis has a maximum value of 10 W m^{-2}, despite a

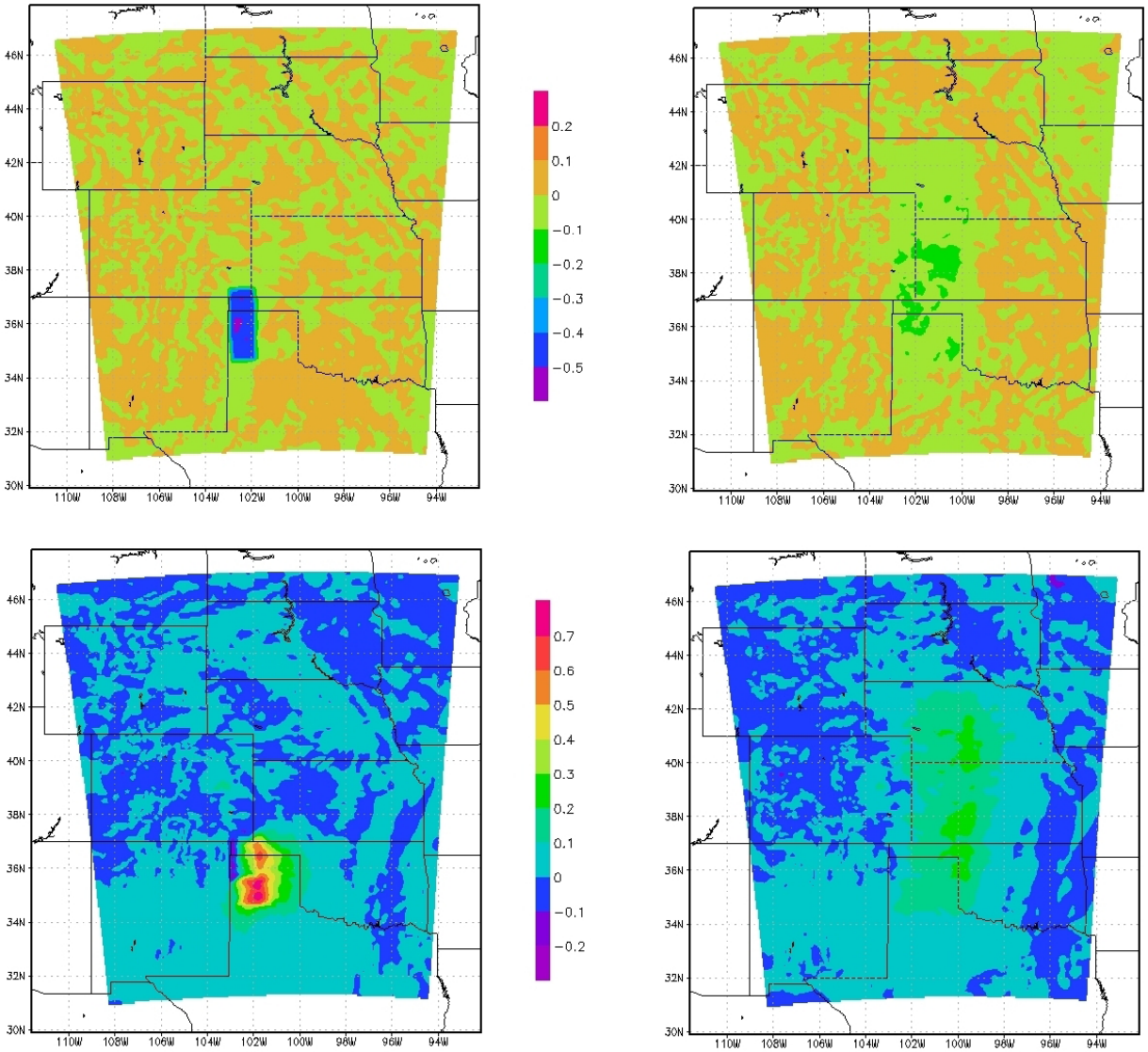

Figure 3. Atmospheric response for two wind farm configurations with similar total capacities but differing capacity density. The left-hand column shows results from a 100 × 300 km wind farm with an installed CD of 4 W m^{-2}, while the right-hand column is for a 300 × 900 km farm with a CD of 0.5 W m^{-2}. The top row shows fractional difference in wind speed cubed between control and wind farms while the bottom two panels show average potential temperature difference (K) at hub height (perturbed-control). Simulations initialized on 5 January 2006 and integrated for 10 days.

max CD of 32 W m^{-2}, which is consistent with the PD expected at that density given the wind speeds in the control run. Each point reflects an individual wind farm simulated with a specific size, location and capacity density. Two wind farms simulated with the same CD, but different spatial size, would have a different expected PD because the winds of the control run will be different despite the same CD. If the wind energy resource could be calculated purely from the observed wind, and was not influenced by other wind turbines, then the points would all lie on the black line. Whereas, we find that PDs drop substantially below a linear model as the expected PD exceeds 1 W m^{-2}, where 'expected PD' is the power density that would be attained if CFs did not decrease with increasing CD. Indeed, for expected PD beyond a few W m^{-2} the addition of more turbines does not result in any additional power production.

Our results suggest that power production as a function on increasing turbine density begins to saturate below 1 W m^{-2} and that it will be difficult to attain large-scale wind power production with a power density of much greater than 1.2 W m^{-2} contradicting the assumptions in common estimates of global wind power capacity [2–4].

The larger wind farm produced a small atmospheric response in terms of not only wind speed reduction, but also magnitude of temperature response in the large array (figure 3). Greater reduction of wind speed in the planetary boundary layer from wind turbines impacts the meteorological fields by changing the natural wind shear. The change to the natural wind shear will lead to increased turbulence generation and promote increased mechanical mixing in the boundary layer. The increased mechanical mixing of the boundary layer (in the absence of a strongly

Table 1. Summary of simulations run and plotted in figure 4. In figure 4, simulations denoted as the same size are plotted with the same symbol (i.e. Small-A, Small-B, and Small-C represent the 3 points plotted as 'small').

Simulation name	Turbine density (number km^{-2})	Capacity density ($W\ m^{-2}$)	Wind farm area (km^2)	Wind farm location	Run period	PBL scheme
Small-A	0.25	0.5	2.7×10^3	See figure 2	5–15 January 2006	YSU
Small-B	2	4	2.7×10^3	See figure 2	5–15 January 2006	YSU
Small-C	8	16	2.7×10^3	See figure 2	5–15 January 2006	YSU
Medium-A	0.25	0.5	3.0×10^4	See figure 2	5–15 January 2006	YSU
Medium-B	2	4	3.0×10^4	See figure 2	5–15 January 2006	YSU
Medium-C	8	16	3.0×10^4	See figure 2	5–15 January 2006	YSU
Large-A	0.25	0.5	2.7×10^5	See figure 2	5–15 January 2006	YSU
Large-B	2	4	2.7×10^5	See figure 2	5–15 January 2006	YSU
Large-C	4	8	2.7×10^5	See figure 2	5–15 January 2006	YSU
Large-D	8	16	2.7×10^5	See figure 2	5–15 January 2006	YSU
Large-E	16	32	2.7×10^5	See figure 2	5–15 January 2006	YSU
X-large-YSU-A	1.25	2.5	2.5×10^5	TX/OK panhandle thru western KS/eastern CO	1 June–1 July 2006	YSU
X-large-YSU-B	1.25	2.5	1.1×10^5	Wyoming	1 June–1 July 2006	YSU
X-large-YSU-C	1.25	2.5	1.3×10^5	South Dakota	1 June–1 July 2006	YSU
X-large-YSU-Total	1.25	2.5	5.0×10^5	All three locations above	1 June–1 July 2006	YSU
X-large-MYJ-A	1.25	2.5	2.5×10^5	TX/OK panhandle thru western KS/eastern CO	1 June–1 July 2006	MYJ
X-large-MYJ-B	1.25	2.5	1.1×10^5	Wyoming	1 June–1 July 2006	MYJ
X-large-MYJ-C	1.25	2.5	1.3×10^5	South Dakota	1 June–1 July 2006	MYJ
X-large-MYJ-Total	1.25	2.5	5.0×10^5	All three locations above	1 June–1 July 2006	MYJ

convective boundary layer) will cause higher potential temperatures to be mixed downward and will result in warming in the lower part of the boundary layer. Figure 3 shows a nearly double warming in the smaller wind farm. This increased warming occurs despite the smaller installed capacity and the smaller energy production. This suggests that the density at which wind turbines are placed within wind farms is important not only for maximizing energy production but also for minimizing environmental impacts. If we consider the environmental impact of large-scale wind farms by looking at the average temperature change times the area impacted, it is plausible that even at a small density large wind farms may still have a relevant environmental impact. In other words, we should not assess the environmental impact as simply the magnitude of the warming, but also by the area impacted by the warming. It is not clear, nor is it the intention of this paper to state, which is a greater environmental impact; the larger magnitude warming over a smaller geographic area or a smaller magnitude warming impacting a larger geographic area.

The magnitude of the temperature changes produced in the model simulations is consistent with those modeled by Roy and Traiteur [28]. Warming of the land surface skin temperature has recently been observed via satellite imagery [29] and the likely process behind the warming was assessed to be due to the mixing created by wind turbine turbulence. However, it is important to note that the warming that will occur due to wind energy turbines, is very different than warming due to green house gases, in that the warming is primarily local, depends on the stability of the atmosphere, and has a finite limit locally in magnitude due to the depth of mixing occurring. The choice of a winter season illustrates the upper bounds of this environmental impact. During summer, especially in regions that experience a convective mixed layer during the day, the warming is much less. When considering possible environmental impacts it is important to look at periods when we expect the biggest impact in order to identify the upper bounds of possible impacts. Note that these impacts may or may not be harmful; our goal is simply to assess their magnitude.

Included on figure 4 are the same calculations for an even bigger wind farm 'X-large'. The X-large wind farm was defined as three separate wind farms; a 2.5×10^5 km^2 area located in Texas and Oklahoma panhandles extending northward into western Kansas and eastern Colorado, a 1.27×10^5 km^2 area in central South Dakota, and a 1.12×10^5 km^2 area in southeastern Wyoming. An installed turbine density of 2.5 $W\ m^{-2}$ was imposed, giving the three large wind farms an installed capacity of 1.2 TW. If the wind farms produced electricity at a capacity factor of 35%, the energy generated would be around 0.42 TW. The X-large wind farm was run for a 30 day period (1 June–1 July 2006), and run with each PBL scheme. The four points plotted for each X-large run represent the actual and expected for each of the wind farms as well as the total. The motivation for running the X-large wind farm simulations was to test important sensitivities; PBL scheme

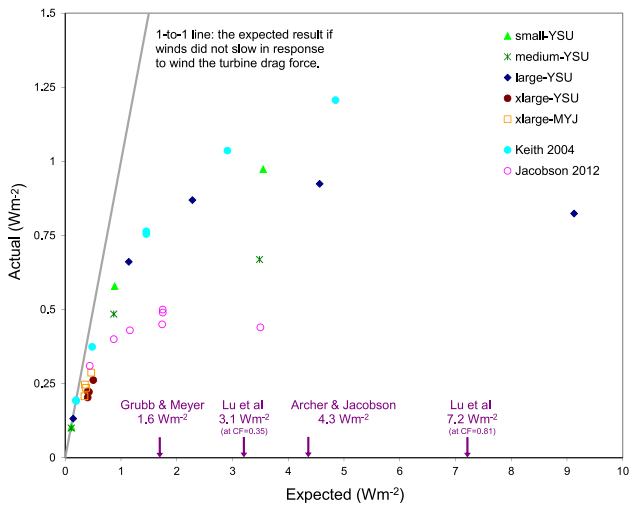

Figure 4. Wind power production predicted by models as a function of the power that would be expected if winds did not change in response to wind turbine induced drag. Data show our simulations using four wind farm sizes and the YSU and MYJ boundary layer schemes as described in the text plotted against winds from a control run with no wind-turbine drag. The grey line shows the linear relationship that would be expected if there was no collective effect. Arrows along the *x*-axis indicate power production density (PD) assumptions made by various estimates of global capacity that do not take into account the collective effects of wind turbine drag. Finally, results from two global model simulations 'Keith 2004' and 'Jacobson 2012' are included as described in the text and in [11, 12] respectively.

chosen, time scale of simulation and meteorological season (summer versus winter). The X-large wind farm results follow the same trend as the small, medium, and large wind farms for the collective effect. This suggests that our results may be independent of the simulation time scale, PBL scheme, and the meteorological season.

Included on figure 4 are results from two different global simulations [11, 12]. Results from Keith *et al* were put into the same framework as the results in this paper for direct comparison. From Jacobson and Archer, the global (100% of world covered in turbines) simulations from their table 1 are plotted[4] in figure 4. The fact that power production saturates around 1 W m^{-2} over in both GCMs and mesoscale models over a range of array sizes spanning more than four orders of magnitude suggests that the result is not likely an artifact of any particular model.

5. Discussion

Results from the mesoscale model described above show that at spatial scales larger than about 100 km^2, extraction of energy by wind turbine arrays is limited by the physics of atmospheric energy transport. The results suggest that the maximum energy that can be extracted by turbine arrays at these scales is about 1 W m^{-2}. This result is surprisingly independent of array size from the small array at 2.7×10^3 km^2 to the 14×10^6 km^2 array used in the GCM study of Keith *et al* [11] to global coverage in Jacobson and Archer [12], and it holds for two different boundary layer parameterizations in the WRF model. We caution against over-interpreting the specific numerical result, however, as it may well depend on factors such as the mean wind speed in the free troposphere overlying the turbine array allowing larger power densities to be extracted (in principle) from regions with stronger winds such as the southern polar ocean.

An immediate implication of this result is that regional analyses of large-scale wind power production, such as Kempton [30], that implicitly assume that capacity factors are independent of total wind capacity will need systematic re-evaluation. Similarly, work that considers how wind resources may change under different climate change scenarios, such as Pryor and Barthelmie [31] will need to take account of the climatic effects of future wind energy deployment.

What then is the global wind resource? There is no simple non-arbitrary way to compute the global wind resource because the presence of large-scale collective effects means that wind resources are not additive. Extracting power in one location alters winds and therefore wind power production in ways that may be non-local and non-linear [11]. A robust estimate of the global wind resource might therefore require one to find the optimal placement of wind power resources in the presence of long-range interactions, a daunting task.

These results suggest that estimates of global wind resource that ignore the impact of wind turbines on slowing the winds may substantially overestimate the total resource. In particular, the results from the three studies [2–4] that estimated wind power capacities of 56, 72 and 148 TW respectively appear to be substantial overestimates given the comparison between model results and the assumptions these studies made about power production densities as shown in figure 4. To cite a specific example, Archer and Jacobson [2] assumed a power production density of 4.3 W m^{-2} yet the results shown in figure 4 (including results from Jacobson and Archer [12]) suggest that production densities are not likely to substantially exceed 1 W m^{-2} implying that Archer and Jacobson [2] may overestimate capacity by roughly a factor of four.

The total wind power capacity can—of course—be very large if one assumes that turbines are placed over the entire land surface or even over the land and ocean surface [12, 13], but while these geophysical limits are scientifically interesting their relevance to energy policy is unclear.

As we discuss in section 2, more policy-driven wind power capacity estimates have restricted the area considered by factors such as wind energy density (e.g., wind power 'class' which impacts production cost), distance from energy demand, or competition with other land uses [2–4]. Yet as shown in figure 4, these estimates have used power production densities that are several times larger than the wind power production limit of around 1 W m^{-2} found in our study and in the global model studies [12, 13]. It is therefore plausible that wind power capacity may be limited to an extent

[4] In order to plot the Jacobson and Archer data, we used the global CF of 31% from the world control run and multiplied it by the turbine installed power density (what we call CD) to get the PD for the *x*-axis. To get the actual PD for the *y*-axis we took the annual total power output and divided it by the earth surface area.

that is relevant to energy policy. Addressing the question demands a new generation of studies that combine realistic physical limits to wind energy extraction with realistic economic and social constraints on wind power siting along with quantification of the climate impacts of wind power extraction.

References

[1] MacKay D J C 2009 *Sustainable Energy—Without the Hot Air* (Cambridge: UTI Cambridge) p 386 (www.withouthotair.com)

[2] Archer C L and Jacobson M Z 2005 Evaluation of global wind power *J. Geophys. Res.* **110** D12110

[3] Grubb M J and Meyer N I 1993 *Renewable Energy: Sources for Fuels and Electricity* ed T B Johansson and L Burnham (Washington, DC: Island) pp 157–212

[4] Lu X, McElroy M B and Kiviluoma J 2009 Global potential for wind-generated electricity *Proc. Natl Acad. Sci. USA* **106** 10933–8

[5] Keith D W 1996 *Energetics. Encyclopedia of Climate and Weather* ed S H Schneider (New York: Oxford University Press) pp 278–83

[6] Peixoto J P and Oort A H 1992 *Physics of Climate* (New York: American Institute of Physics)

[7] Best R W B 1979 Limits to wind power *Energy Conversion* **19** 71–2

[8] Wiser R and Bolinger M 2007 *Annual Report on US Wind Power Installation, Cost and Performance Trends: 2006*

[9] Apt J 2009 Carnegie Mellon, personal communication

[10] DOE/EIA-0554, 2009, available at: www.eia.doe.gov/oiaf/aeo/assumption/pdf/renewable.pdf

[11] Keith D W *et al* 2004 The influence of large-scale wind power on global climate *Proc. Natl Acad. Sci. USA* **101** 16115–20

[12] Jacobson M Z and Archer C L 2012 Saturation wind power potential and its implications for wind energy *Proc. Natl Acad. Sci. USA* **109** 15679–84

[13] Marvel K, Kravitz B and Caldeira K 2012 Geophysical limits to global wind power *Nature Clim. Change* **3** 118–21

[14] Wang C and Prinn R 2009 Potential climate impacts and reliability of very large wind farms *MIT Joint Program on the Science and Policy of Global Change Report No.* 175

[15] Kirk-Davidoff D B and Keith D W 2008 On the climate impacts of surface roughness anomolies *J. Atmos. Sci.* **65** 2215–34

[16] Baidya Roy S, Pacala S W and Walko R L 2004 Can large windfarms affect local meteorology? *J. Geophys. Res. Atmos.* **109** D19101

[17] Rooijmans P 2004 Impact of a large-scale offshore wind farm on meteorology: numerical simulations with a mesoscale circulation model *Masters Thesis* Utrecht University, Utrecht

[18] Barrie D B and Kirk-Davidoff D B 2009 Weather response to management of a large wind turbine array *Atmos. Chem. Phys. Discuss.* **9** 2917–31

[19] Fiedler B H and Bukovsky M 2011 The effect of a giant wind farm on precipitation in a regional climate model *Environ. Res. Lett.* **6** 045101

[20] Fitch A C, Olson J B, Lundquist J K, Dudhia J, Gupta A K, Michalakes J and Barstad I 2012 Local and mesoscale impacts of wind farms as parameterized in a mesoscale NWP model *Mon. Weather Rev.* **140** 3017–38

[21] Adams A S and Keith D W 2007 Wind energy and climate: modeling the atmospheric impacts of wind energy turbines *Eos. Trans. Am. Geophys. Union* **88** (Fall Meeting Suppl.) Abstract B44B-08

[22] Skamarock W C, Klemp J B, Dudhia J, Gill D O, Barker D M, Wang W and Powers J G 2005 A description of the advanced research WRF version 2 *NCAR Tech Notes-468+STR*

[23] Janjic Z I 2002 Nonsingular implementation of the Mellor–Yamada Level 2.5 scheme in the NCEP Meso model *NCEP Office Note No. 437* p 61

[24] Hong S-Y, Yign N and Jimy D 2006 A new vertical diffusion package with an explicit treatment of entrainment processes *Mon. Weather Rev.* **134** 2318–41

[25] www.wasp.dk/Download/PowerCurves.html

[26] Lin Y-L, Farley R D and Orville H D 1983 Bulk parameterization of the snow field in a cloud model *J. Appl. Meteorol.* **22** 1065–92

[27] Barthelmie R J, Pryor S C, Frandsen S T, Hansen K S, Schepers J G, Rados K and Schlez W 2010 Quantifying the impact of wind turbine wakes on power output at offshore wind farms *J. Atmos. Oceanic Technol.* **27** 1302–17

[28] Roy S B and Traiteur J J 2010 Impacts of wind farms on surface air temperatures *Proc. Natl Acad. Sci. USA* **107** 17899–904

[29] Zhou L, Tian Y, Roy S B, Thorncroft C, Bosart L F and Hu Y 2012 Impacts of wind farms on land surface temperature *Nature Clim. Change* **2** 539–43

[30] Kempton W, Pimenta F M, Veron D E and Colle B A 2010 Electric power from offshore wind via synoptic scale interconnection *Proc. Natl Acad. Sci. USA* **107** 7240–5

[31] Pryor S C and Barthelmie R J 2011 Assessing climate change impacts on the near term-stability of the wind energy resource over the United States *Proc. Natl Acad. Sci. USA* **108** 8167–71